Review

Research Requirements to Move the Bar forward Using Aqueous Formate Salts as H₂ Carriers for Energy Storage Applications

Katarzyna Grubel [1, *], Ji Su [2], Jotheeswari Kothandaraman [1], Kriston Brooks [1], Gabor A. Somorjai [2], Tom Autrey [1]

1. Pacific Northwest National Laboratory, 902 Battelle Boulevard, P.O. Box 999, Richland, Washington 99352, United States; E-Mails: katarzyna.grubel@pnnl.gov; jotheeswari.kothandaraman@pnnl.gov; Kriston.Brooks@pnnl.gov; tom.autrey@pnnl.gov
2. Materials Sciences Division, Lawrence Berkeley National Laboratory, Berkeley, California 94720, United States; E-Mail: jisu@lbl.gov; somorjai@berkeley.edu

* **Correspondence:** Kat Grubel; E-Mail: katarzyna.grubel@pnnl.gov

Academic Editor: Alfonso Chinnici

Abstract

In this perspective on hydrogen carriers, we focus on the needs for the development of robust active catalysts for the release of H₂ from aqueous formate solutions, which are non-flammable, non-toxic, thermally stable, and readily available at large scales at reasonable cost. Formate salts can be stockpiled in the solid state or dissolved in water for long term storage and transport using existing infrastructure. Furthermore, formate salts are readily regenerated at moderate pressures using the same catalyst as for the H₂ release. There have been several studies focused on increasing the activity of catalysts to release H₂ at moderate temperatures, i.e., < 80 °C, below the operating temperature of a proton exchange membrane (PEM) fuel cell. One significant challenge to enable the use of aqueous formate salts as hydrogen carriers is the deactivation of the catalyst under operating conditions. In this work we provide a review of the most efficient heterogeneous catalysts that have been described in the literature, their proposed modes of deactivation, and the strategies

reported to reactivate them. We discuss potential pathways that may lead to deactivation and strategies to mitigate it in a variety of H$_2$ carrier applications. We also provide an example of a potential use case employing formate salts solutions using a fixed bed reactor for seasonal storage of energy for a microgrid application.

Keywords
Formate salts; hydrogen storage; hydrogen carriers; catalyst deactivation; catalytic hydrogen production

1. Introduction

In light of the need for large scale, geographically agnostic approaches to store energy, hydrogen and hydrogen carriers in particular are receiving increased scientific attention [1-3]. Since compressed, or liquified, hydrogen is inherently challenging to handle, there is a pressing need for development of hydrogen carriers that would alleviate hydrogen loss due to leaks or evaporation, and liquid organic hydrogen carriers (LOHCs) fulfill this requirement. LOHCs are molecules that contain chemically bound hydrogen that can be released when external stimuli are applied. Current research concentrates on methylcyclohexane (MCH), perhydro-*N*-ethylcarbazole (H12-NEC), and perhydro-dibenzyltoluene (H18-DBT), which can deliver three, six, and nine molecules of H$_2$, respectively. Comparison of important characteristics of LOHCs is shown in Table 1 [4].

Table 1 Comparison of currently considered LOHCs.

	H₂ capacity (g/kg)	H₂ storage density at RT (g/L)	Density (20 °C) (kg/m³)	Melting Point (°C)	Boiling point at 1,013 hPa (°C)	GHS Symbol
Perhydro-NEC	58 (1.9 kWh/kg)	58 (~1.8 kWh/L)	~900-1000	<20	~280	N/A
NEC	-	-	Solid	~68	270	[GHS07]
Methylcyclohexane	62 (2.06 kWh/kg)	47 (~1.59 kWh/L)	770	-126	110	[GHS07] [GHS02] [GHS09] [GHS08]
Toluene	-	-	870	-95	111	[GHS07] [GHS02] [GHS08]
Decalin	73 (2.4 kWh/kg)	64 (2.1kWh/L)	880	-43	189-191	[GHS01] [GHS02] [GHS09] [GHS08] [GHS06]
Naphthalene	-	-	1140	80.3	218	[GHS07] [GHS02] [GHS08]
Benzyltoluene	62 (2.06 kWh/kg)	56 (1.66 kWh/L)	995	-70	285	[GHS07] [GHS08]
Perhydrobenzyltoluene	-	-	~905	-30	~270	[GHS07] [GHS08]
DBT	62 (2.06 kWh/kg)	58 (1.94 kWh/L)	1040	-34	390	[GHS08]
PerhydroDBT	-	-	920	-45	370	[GHS08]
Formic Acid*	43 (1.45 kWh/kg)	53 (1.77 kWh/L)	1220	8.4	100.8	[GHS02] [GHS06] [GHS05]

* Decomposes to H_2 and CO_2.

Despite of the high hydrogen content (5.8 wt. % (64 g H_2/liter) and 6.2 wt. % (67 g H_2/liter), for H12-NEC and H18-DBT, respectively), these LOHCs require higher temperatures to enable release of hydrogen. As such, there is continued interest in development of new hydrogen carriers that will release hydrogen at lower temperatures. The example we focus on in this work are formate salts HCOOM (M = Li^+, Na^+, K^+, Cs^+, NH_4^+), which present an alternate approach to storing and transporting large quantities of H_2 safely and economically, releasing hydrogen in the presence of a catalyst at temperatures ≤ 80 °C [5-13]. Moreover, synthesis of formate salts may be accomplished by reduction of CO_2 molecules, which could contribute to lowering carbon footprint [14-19]. Formate salts are non-toxic, non-flammable and, compared to compressed or liquified hydrogen, are inherently more stable and easier to handle. For applications where the volumetric and gravimetric footprint of the storage system is not as critical as cost, e.g., a microgrid neighbourhood or emergency backup power for a data centers, stability and safety could tip the balance toward these compounds.

It is notable that ½ of the H_2 release from aqueous formate solutions comes from water and the by-product is bicarbonate. While limited solubility of bicarbonate and its potential precipitation in reactor may present challenges, engineering controls can be used to alleviate this problem. Comparison of important parameters between formate salts is given in Table 2.

Table 2 Comparison of features between formate salts.

	Aqueous Formate Salts			
	HCOONa	HCOOK	HCOOCs	$HCOONH_4$
Product of dehydrogenation	H_2, $NaHCO_3$	H_2, $KHCO_3$	H_2, $CsHCO_3$	H_2, NH_4HCO_3
Solubility of products in H_2O	Low (solids)			
$\Delta_r G^0$ for dehydrogenation* (kJ/mol)	1.4	1.3	N/A	+1.5
$\Delta_r H^0$ for dehydrogenation* (kJ/mol)	20.4	19.3	N/A	+19.4
Volumetric density and concentration of formate (H_2 in aqueous carrier at 80 °C (g/L)#	16.8	34.2	N/A	32.3
Gravimetric density of formate (H_2 in carrier at 80 °C (g/kg)#	13.2	20.3	N/A	26.7
Formula weight (g/mol)	68	84	178	63
Density (g/cm³)	1.9	1.9	2.4	1.3
Hydrogen capacity of solid (g H_2/L)	56.5	45.5	27.0	40.6
Solubility (g of formate salts/1000 g H_2O @ 20 °C)	812	3370	4500	1430
Total mass of 1L of saturated solution (g)	1812	4370	5500	2430
wt. % of formate salts at saturation	45	77	82	59
Specific gravity at wt. %	1.3	1.6	2.3	1.2&

|				
Total volume of saturated solution (mL)	1426.8	2731.2	2391.3	2025
Upper limit volume of saturated formate solution (mL)	1422.9	2764.4	2875.0	2117.2
g H_2/L of solution	16.7	29.4	21.1	22.4

* Theoretical values.

\# Considering mass of water - based on solubility limit of corresponding formate salt: 8.4 M, 17.1 M and 16.2 M, respectively.

\& Estimated.

N/A = not available.

While there are many advantages of using formate salts and the aqueous solutions of formate salts, such as non-flammability, ease of transport and non-toxicity, there are also challenges that need to be addressed. Namely, decreased solubility of the product of dehydrogenation and the limitation of maximum achievable H_2 pressure, which is governed by the equilibrium. It is helpful therefore to introduce several concepts that allow for direct comparison of amount hydrogen that is available [20]. These are: *storage capacity*, *deliverable capacity*, and *usable capacity* (Figure 1). Storage capacity is limited by the amount of H_2/L of formate salt; deliverable capacity is limited by solubility of formate salt at ambient temperature; usable capacity is limited by the solubility of bicarbonate salt at temperature of reaction.
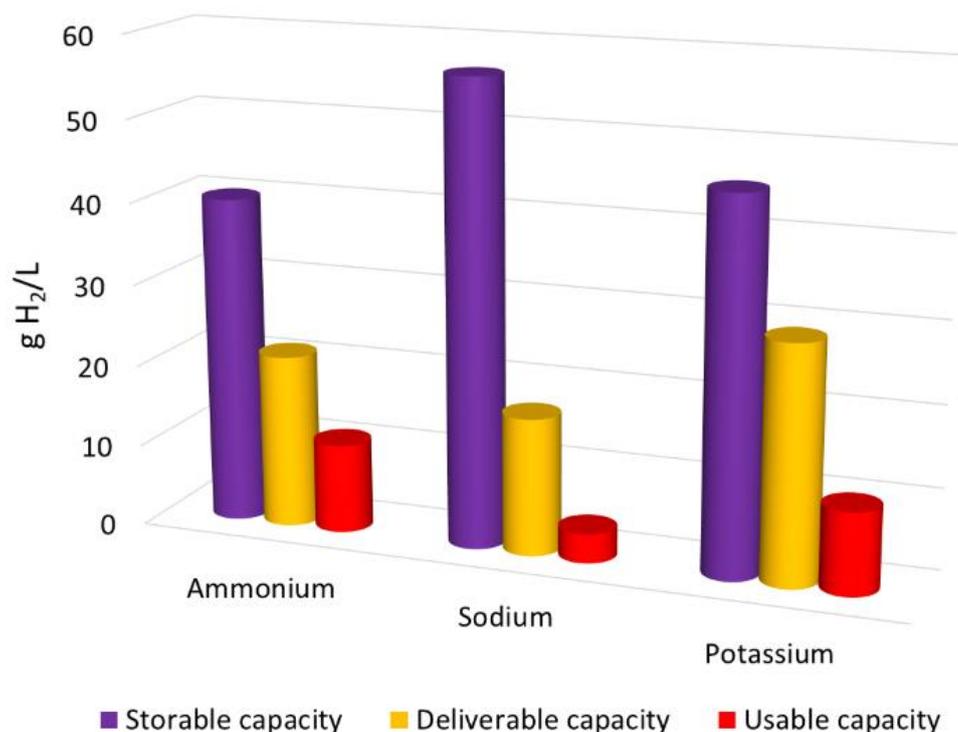
Figure 1 Visual representation of *Storable*, *Deliverable*, and *Usable* Capacities.

The degree of hydrogen release from formate salts is governed by the equilibrium, and one cannot obtain high pressures of released hydrogen. Despite these challenges, we envision that

formate salts can be used as H$_2$ carriers where a steady stream of hydrogen is needed, and compression of H$_2$ is not required. As H$_2$ carriers are considered for applications beyond onboard H$_2$ storage for fuel cell electric vehicles (FCEV), there is growing recognition that there is no "one size fits all" approach for all potential applications. For example, there is an interest in using H$_2$ as a reductant in the steel industry [21-23], where H$_2$ purity is not so critical as it is for a PEM fuel cell. Additional advantage of formate salts as H$_2$ carriers is that the by-product, bicarbonate, can be readily hydrogenated to regenerate the formate under moderate temperatures <60 °C and H$_2$ pressures <20 bar, or can be regenerated electrochemically without production of hydrogen (Scheme 1) [16].
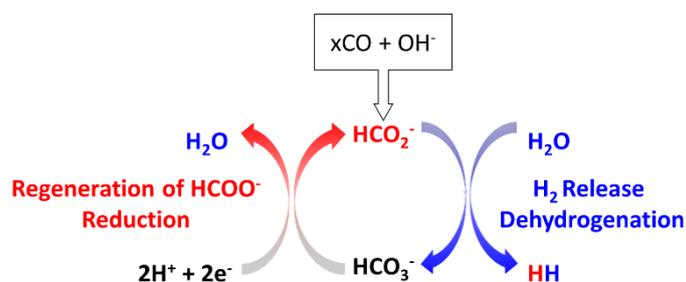
Scheme 1 Energy Cycle Based on Formate/Bicarbonate Cycle.

Worldwide demand for formates is growing, and for sodium formate is projected to reach up to 4.5 % annual growth rate during 2019-2027 [24]. Industrially, sodium formate is synthesized by reacting sodium hydroxide with excess of carbon monoxide (CO) under 17-19 bar and 150 °C – 220 °C [25]. The key factor driving demand for sodium formate is its potential use as an organic feed additive, environmentally-friendly deicer, and its use in textile and printing industries. This increased demand for formates has driven down its market price and in 2020, a metric ton was priced at $368. Considering this price and hydrogen content in sodium formate, one can estimate that the *first fill* for one kg of H$_2$ would cost $12.5, not accounting for cost of all transformations required. Subsequent cost would depend on cost of regeneration of formate from the bicarbonate salt. While the cost of the first fill is lower than the average retail price of H$_2$ for the light duty vehicles ($16.54), as estimated by California Energy Commission [26], it is greater than the DoE target of levelized cost of H$_2$ $2.30/kg H$_2$ [27]. Thus, focused technological advancements in regeneration step are needed to meet this milestone. However, if one considers interseasonal, long-term storage, formate salts offer a distinct advantage of presenting no H$_2$ losses. Additionally, they can be stored either as solid or aqueous solution in vessels that do not require any reinforcement, or expensive modifications.

In this perspective we review what has been reported in terms of (i) heterogeneous catalyst activity in aqueous solutions of formates, describing catalyst properties that appear to enhance rates of H$_2$ release, and (ii) catalyst stability; i.e., the properties that that may lead to catalyst deactivation. We describe remaining challenges and offer potential research directions to address them and move the bar forward. While we recognize that there are reports of homogeneous catalysts that appear to be more stable and exhibit higher turnover numbers compared to heterogeneous catalysts, we focus this perspective on heterogeneous catalysis as this provides an opportunity to describe a use case scenario where a system of formate salts is used to store renewable energy generated in a microgrid powered neighbourhood.

2. Catalytic Activity

There is an abundance of information describing the correlation between the type of metal and its effectiveness as a catalyst in the rate of decomposition of formic acid (FA) and mixtures of FA and formate salts [20] however, there is comparatively less data available describing the effectiveness of monometallic catalysts for H_2 release from aqueous formate salts. The information available can be summarized as 1) palladium (Pd) is more effective than other metals, 2) Pd on a carbon support is better than an Pd on oxide support, 3) Pd on carbon doped with nitrogen is better than undoped carbon, and 4) Pd nanoparticles between 2-3 nm are better than larger Pd nanoparticles [10-13, 28].

A notable exception appears to be the recent report that platinum nanoparticles dispersed on polyvinylpyrrolidone are competent catalyst for decomposition of formate salts [29]. Similarities between the Pd and Pt nano catalysts are that 1) there is an optimum pH range for formate dehydrogenation, and 2) the catalyst deactivation mechanism is not fully understood. One can argue that it is the nature of the rate determining step (RDS) that allows Pd catalyst to perform better during dehydrogenation of formate salts. It has been shown that the electronic interactions between hydrogen atoms vary depending on the nature of metal and are repulsive in case of the Pd surface, while being almost non-existent in case of Pt [30].

As already stated, combination of Pd and carbon support is generally most active toward formate dehydrogenation. A 5 wt. % Pd/C is ~5 times more active for potassium formate (initial Turnover Frequency, iTOF, of 1241 h^{-1}) than the Pd on metal oxide supports such as TiO_2 (iTOF=204 h^{-1}) and Al_2O_3 (iTOF=285 h^{-1}) under the same experimental conditions and metal loading (note that the surface area of the supports are not given) [7]. While CO poisoning is identified as a possible cause of catalyst deactivation in the FA dehydrogenation in the presence of oxide supported metal catalysts [31], it is not the case in the formate dehydrogenation. Likewise, with the carbon-based supports, when metals such as Au, Ir, Pt, Ru and Rh are used instead of Pd, the catalysts are inactive for formate dehydrogenation [7]. It is important to note that the same trend is observed for the reverse reaction i.e. hydrogenation of bicarbonate to formate [13]. It has been also shown that Pd and carbon combination is the best catalyst for ammonium bicarbonate hydrogenation compared to Pd/Al_2O_3, $Pd/CaCO_3$, $Pd/BaSO_4$, Ru/AC, Rh/AC, Pt/AC (inactive), and Ni/AC (inactive) [13]. Better dispersion of Pd on the activated carbon (AC) support and local enrichment of H_2 (by H_2 spillover effect) from Pd to support are identified as potential reasons for superior activity of Pd on C compared to other supports in the case of bicarbonate hydrogenation.

Many modifications were performed on the carbon supports to further improve the catalyst's activity toward formate dehydrogenation. The carbon-based supports such as reduced graphite oxide (r-GO) nanosheets [7], N-doped mesoporous carbon [11, 28], and chitosan-graphene oxide beads [5] gave better catalytic activity than the commercial Pd/C catalyst. In the case of r-GO support, the catalytic activity is highly dependent on the lattice strain of the Pd at the interface [7]. Highly strained Pd nanoparticles gave high activity, which was confirmed by the correlation between the lattice strain (of commercial 5 wt.% Pd/C, 5 wt. % Pd/r-GO, 2 wt. % Pd/r-GO, and 1 wt. % Pd/r-GO) and the iTOF values. In the case of N-doped carbon supports, the doped nitrogen provides Lewis basic sites and prevent the particle aggregation and overgrowth, which was observed for both FA [32, 33] and formate dehydrogenation [11]. Table 3 shows the iTOF reported in the literature for some of the most active heterogenous Pd-catalyzed formate dehydrogenation

at 80 °C. The state-of-the-art catalyst gives an iTOF of 11,300 h^{-1} (Table 3, entry 1) for dehydrogenation of 5 mL of 4.8 M potassium formate solution. A H$_2$ yield of 96% is obtained after 2 h, which results in a total TOF of 3750 h^{-1}. Based on the metal content in the catalyst, in order to produce one kg of hydrogen *per* minute from 4 M potassium formate solution, 0.891 kg of Pd metal is required. The Pd/r-GO catalyst is more active for potassium formate dehydrogenation compared to sodium formate, lithium formate, and ammonium formate dehydrogenation. The activity toward formate dehydrogenation, given in the decreasing order, is as follows: potassium formate > sodium formate > ammonium formate > lithium formate. Similarly, using a commercial Pd/C catalyst, and based on the iTOF of 3200 h^{-1}, 1.077 kg of Pd would be required to produce a kg of H$_2$/min from 7 M sodium formate solution. When a 92% H$_2$ yield is achieved, the total TOF of the reaction is ~1096 h^{-1}, which would require 3.144 kg of Pd to release a kg of H$_2$/min. Among the formate salts (potassium formate, sodium formate and ammonium formate) screened using commercial Pd/C catalyst, ammonium formate provided the best TOF and H$_2$ yield. However, dehydrogenation of ammonium formate also resulted in release of ammonia vapours, which will have to be removed if the gas stream is to be delivered to the PEM fuel cell.

Table 3 Pd-catalyzed formate dehydrogenation at 80 °C.

Entry	Catalyst	Substrate	iTOF (h^{-1})	H$_2$ yield (%)	Time (min)	Ref.
1	1 wt. % Pd/r-GO	4.8 M HCOOK	11,300 [a]	96	120	[7]
2	4.6 wt. % Pd/NMC-8	2 M HCOOK	2,416 [b]	55	60	[32]
3	3 wt. % Pd/C	7 M HCOONa	3,200 [b]	92	100	[34]
4	5 wt. % Pd/AC	1 M HCOONH$_4$	2,135 [b,c]	77	40	[13]

[a] Initial TOF calculated from first 20 min.
[b] Initial TOF calculated from first 10 min.
[c] Initial TOF calculated based on surface active site.

3. Catalyst Stability

The information on the stability of the catalysts used to release hydrogen from formate salts is sparse. Careful investigation of more complete experimental studies shows that most of the heterogeneous catalysts reported to date are reactivated after each batch use and most of them can be reactivated with simple procedures (described below). This is fortunate given the high price of Pd, which has been growing steadily since it started to be traded. In mid-90s, the price was hovering around $5000/kg. As of the time of this article, the price was steady ~$70,000/kg. One needs to consider that this is just Pd metal and additional costs will be incurred during its conversion to various forms and catalysts. Additionally, Pd is about 30 times rarer than gold, which makes any losses in metal, or catalyst, activity of Pd-based catalyst costly and not economically viable.

In terms of catalyst longevity for formate dehydrogenation, commercial Pd/C was shown to perform well up to fifteen reversible cycles in 4 M HCOOK-KHCO$_3$ system [8]. The authors also pointed out that subsequent hydrogenation of the dehydrogenation by-product (bicarbonate)

prevented the catalyst deactivation and no obvious catalyst deactivation is mentioned. This could explain why the drop in the activity was observed when the Pd/C catalyst was used only for the continuous potassium formate dehydrogenation instead of cyclic transformation of formate-bicarbonate [34]. Similarly, in the case of cyclic transformation of $HCOONH_4$-HCO_3NH_4 system, there is no drop in the activity observed over five cycles in the presence of commercial Pd/AC catalyst [13]. Although the modified carbon supports (such as r-GO, N-doped mesoporous carbon) are known to exhibit better catalytic activity than Pd/C, the longevity of these catalysts was not studied for more than 6 cycles [7, 11]. To the best of our knowledge, performance of catalysts for formate salts dehydrogenation are only tested in batch reactors and never for continuous flow through operation.

While from an academic point of view turnover frequency (TOF) is often quoted as the most important feature of the catalyst, in industrial settings, catalyst stability, i.e., turnover number (TON), may be more important. If faster rates of H_2 release are needed, the amount of catalyst can be adjusted. However, because of the magnitude of operations, it is often not feasible to exchange the spent catalyst after every batch reaction.

Given all the benefits of using formate salts to store and transport hydrogen it is surprising that there is very little effort to understand what process or processes are leading to catalyst deactivation. To this end, we propose several possibilities that could be changing over the course of a reaction. But first we describe how deactivated catalysts are regenerated. This insight could be useful in understanding how the best Pd on carbon supported catalysts are deactivated in such short order.

Additionally, while laboratory operations can be easily performed in small batches, industrial reactions are very often performed in continuous fashion using flow reactors. Also, unlike in the fundamental research, industrially, the most important metrics are space-time yield (STY) and catalyst productivity [35].

$$\text{STY} = \text{gram}_{\text{product}} \, [\text{cm}^{-3}] \, _{\text{reactor volume}} \, [\text{hour}^{-1}]$$

$$\text{Catalyst productivity} = \text{gram}_{\text{product}} \, [\text{kg}^{-1}] \, _{\text{catalyst}} \, [\text{hour}^{-1}]$$

Considering the above, it is imperative to address how the understanding of catalyst deactivation in laboratory setting can be translated into the larger scale industrial operations. One of the drawbacks for this translation is the way the stability tests are performed. Typically, in small research operations, after each batch reaction is performed, spent catalyst is separated from the reaction mixture and reused in the next batch of reactions. Separation of the catalyst may further involve various treatments of the catalyst between catalytic runs. Here, we will discuss treatment of spent heterogeneous Pd catalysts obtained during aqueous dehydrogenation of formate salts, and how this treatment can be handled in the industrial settings.

Laboratory research on aqueous formate salts as H_2 carriers concentrates on development of catalytic materials that have the potential to reduce costs, increase reaction rates, and provide efficient catalytic cycling. As mentioned earlier, Pd nanoparticles supported on carbon-based materials are the most promising candidates, as they exhibit the highest activity and stability. It needs to be pointed out that the assessment of degree of catalyst deactivation should be based on the initial rates. While it is possible that the TON may remain the same in consecutive catalytic runs, differences in the initial rates suggest that the catalyst undergoes modifications during

catalytic process. Therefore, we recommended that the initial reaction rate be used as an indicator of catalyst deactivation.

Generally speaking, catalyst deactivation is a result of a change in the local environment of the active site. For a low temperature aqueous phase reaction such as formate dehydrogenation, chemical or physical changes of the active Pd center may influence one or more steps in the heterogenous reaction including diffusion, adsorption, activation of the reactants, and/or the desorption and diffusion of the products. Based upon the reaction process and structure-activity relationship reported in the literature, we summarize and discuss some of the reasons for deactivation of Pd catalyst in the formate/bicarbonate cycle.

In case of hydrogen release from aqueous formate solutions, the most common workup of spent catalyst includes washes with various media (ultrapure water being the most common) and drying either at elevated temperature, or under vacuum. Curiously, this treatment has been reported even in cases when the growth of Pd nanoparticles was cited as the main deactivation pathway of the catalyst [5, 10]. It has been suggested that the optimal size of the nanoparticles is in the range of about 2 nm and the growth/agglomeration beyond 3 nm contributes to decreased reactivity. Therefore, a highly dispersed and strained Pd nanoparticle anchored on carbon support is one of the key factors influencing activity of the catalyst. This theory is supported by the fact that catalysts with surface modifications designed for more permanent attachment of particles on the surface show no growth of the nanoparticles [36]. This kind of particle growth may be a result of either Ostwald ripening or particle migration and coalescence, and results in the loss of the active surface area [37]. Ostwald ripening involves migration of adatoms, which is the result of differences in surface energy and includes dissolution of small particles and their re-deposition [38]. Particle migration and coalescence on the other hand is the result of Brownian-like motions on the supporting surface. It can be postulated that during Ostwald ripening, one could detect metal particles dissolved in the reaction mixture, however there are no reports of such detection. This may point to the particle migration and coalescence being responsible for growth of the particles. Another explanation that has been reported in literature is that even at low temperature headspace atmosphere, liquid water, and pH have strong impact on metal dispersion [39-41]. It has been shown that the low pH contributes to catalyst sintering [39]. However, dehydrogenation of formate salts is performed under alkaline conditions, which is not expected to contribute to the sintering.

Additionally, while CO poisoning is identified as a possible cause of catalyst deactivation in the FA dehydrogenation in the presence of oxide supported metal catalysts [31], it is not the case in the formate dehydrogenation. It was suggested that the CO formation during dehydrogenation of formate could lead to additional poisoning of the catalyst. There are two factors against this suggestion. First, dehydration of formate salts, which would lead to formation of metal-bound CO was observed on Ni(110), Ni(100), Ni(111), Fe(100), Ru(100), and Ru(001) surfaces only [42], where it was investigated as an intermediate step during methanol synthesis and water-gas shift (eq. 1). Second, if CO was indeed poisoning the catalyst, simple solvent wash would not be effective in restoring catalytic activity. While it is possible that small amounts of CO are formed during reverse water-gas shift, to date, there are no reports of detection of CO during decomposition of formate salts.

$$CO + H_2O \leftrightharpoons CO_2 + H_2 \qquad\qquad (eq.\,1)$$

Another possible mode of deactivation of the catalyst could be change in oxidation state of active metal. It has been shown that during dehydrogenation of ammonium formate initial mixture of Pd(0)/Pd(II) is converted entirely to Pd(0) [13]. This result was recorded after one cycle of dehydrogenation of formate/hydrogenation of bicarbonate, and the catalyst was shown to be active in four additional cycles. A similar result was reported for a Pd catalyst in dehydrogenation of FA. This indicates that the change in oxidation state of active metal may not be responsible for loss of activity of the catalyst. It is viable however, that the changes in the oxidation state of metal would trigger additional changes in the catalyst, leading to modification of local electronic structure and defects. These changes could take place on the same time scale as the growth of the particles and be closely connected. In such case, there might be significant electronic effects, which affect the binding energy between catalyst, reactants, and products, and inhibit facile product release [43].

Catalytic activity of Pd nanoparticles is determined in part by the nature of the support on which the metal has been deposited. In general, chemical nature of the surface of activated carbon can play critical role in adsorption process and catalytic transformations. The major functionality on a carbon surface can be introduced by oxygen-containing functional groups (OCFGs) such as carboxyl, carbonyl, and hydroxyl. These OCFGs can provide active sites for selective adsorption of species from solutions and change the hydrophobicity of the carbon surface. The OCFGs on carbon surface also increase dispersion of the metal nanoparticles [44] e.g., dispersion of Pd nanoparticles on AC is higher than that on other supports such as Al_2O_3, $CaCO_3$, and $BaSO_4$. This dispersion implies presence of increased number of active Pd sites available for hydrogenation/dehydrogenation [45].

The OCFGs can also influence diffusion and elimination of hydrogen from the Pd surface. As formate dehydrogenation/bicarbonate hydrogenation is a multiphasic reaction (gas/liquid/solid), diffusion of the reactants, products, or H_2, could be rate limiting. Activated carbon is commonly used as a hydrophobic support that can also store H_2 [46-48], a feature that can be enhanced by the presence of OCFGs [48], which modify electronic structure of support and stabilize Pd nanoparticles. Therefore, the hydrogen storage property of carbon support and H_2 spillover effect between the support and Pd surface may play role in the catalytic performance.

It has been postulated that in the case of FA, formate ions can act as catalyst poisons by blocking catalyst pores [49]. This assertion was made based on the observation that stirring of the catalyst with solution of sodium formate decreased catalyst activity in dehydrogenation of FA. Similar observation was made by Jeong *et al.* [34], where pre-stirring of the Pd/C catalyst with sodium formate decreased the volume of released H_2 from the formate salt. On the other hand, the authors of this publication have shown that the product of formate dehydrogenation (sodium bicarbonate) does not exhibit similar inhibitory effect by stirring the catalyst with bicarbonate salt prior to attempting FA dehydrogenation. The authors conclude that there is a potential "poison" in the reaction mixture as well as a growth in size of the active particles and subsequent deactivation of the catalyst. This is not the case in the publication of Caiti *et al.*[49], where particle size is reported to be unchanged between fresh and used catalyst, but decreases after washing the catalyst with water. A common observation, however, is that the particle distribution is much wider after dehydrogenation reaction, a dependency which was also observed by Wang *et al*. [10].

In light of all these observations it is plausible that more than one mode of deactivation may be operational. This assertion is based on the fact that it is a common practice to wash the catalyst

between uses regardless of any other changes taking place with catalyst, however two deactivation modes outlined below need to be considered:

1) If catalyst deactivation was due to the fouling of the pores only, as suggested by Caiti *et al.*, washing of the catalyst would fully restore catalyst activity and could be repeated indefinitely. Yet, it has been shown that the catalyst activity decreases after five or six cycles [49].

2) If growth of the particles was the only cause of deactivation, repeated washing of the catalyst with solvents would not re-establish even partial reactivity.

It is entirely possible that both processes (fouling and particle growth) take place at the same time, and over shorter periods of time (several catalytic runs) fouling exerts more prominent effect, but with the repeated use of the catalyst, particle growth and electronic changes are becoming more prominent in deactivation. That kind of pathway would be reasonable, as during the initial uses washing out catalytic poison would restore reactivity, but it would not mitigate the permanent change in the size of the particles, which may be slow to occur.

A possible mitigation tactic in designing new catalysts based on Pd nanoparticles may be synthesis of a support decorated with moieties that better spatially disperse and anchor Pd particles and prevent their movement and migration. One of such catalysts have been reported in 2015 by Song *et al.* and includes diamine moieties decorating r-GO [36]. This catalyst has been developed for dehydrogenation of FA/sodium formate mixtures and was shown to be active over five cycles without drop of activity. This validates the approach which emphasizes immobilization of particles to prevent their migration. In such case, if any regeneration is needed, it can be reasonably assumed that engineering controls can be applied to accomplish that.

4. Reactor Design

As discussed in previous sections, the dehydrogenation product of formate salt is the corresponding bicarbonate, which is less soluble at reaction temperature. Therefore, it becomes imperative that this product does not accumulate in the catalyst bed and block active sites. It could be envisioned that washing of the catalyst may utilize either fresh batch of water (or other solvent), or water from the fuel cell reaction as discussed elsewhere in this article.

Regeneration of catalyst is a common issue for a range of hydrocarbon-based catalytic reactions. Reactions such as hydrotreating of naphtha [50], alkylation of aromatics [51], and deoxygenating hydrocarbons [52] experience coking and the catalysts used in these processes can be regenerated by burning off the coke with air and can be accomplished by a variety of methods [53]. The bed can be taken offline and regenerated in place with air, inert gas and elevated temperatures. Once regeneration is complete, the catalyst can be brought back online for continued operation. Alternatively, a continuous catalyst regeneration (CCR) scheme can be used. In this case, one or more reactors are stacked with a moving bed of catalyst that trickles from the top of the first reactor to the bottom reactor by gravity. The partially deactivated catalyst from the bottom of the reactor stack is continuously withdrawn and transferred to a regenerator, and then sent back to the top of the first reactor section. Additionally, fluidized bed reactors also allow regeneration by removing a fraction of the catalyst either at the top or bottom of the bed during reaction. Freshly regenerated catalyst is then fed continuously to the reactor bed. Next, it is discharged either through an overflow pipe, or by entrainment for regeneration. Each of these

three reactor designs, or similar engineering solution, could be used for the regeneration of catalyst during dehydrogenation of formate salts.

One of the simplest approaches that we propose would be a switchable array of trickle-bed reactors with countercurrent gas flow, which can be the most advantageous to this process. This configuration would allow for optimizing the liquid-to-gas ratio and will enable continuous dehydrogenation process, where half of the array is accomplishing dehydrogenation and the other half of catalytic beds is being regenerated. Since there are no reported studies on the continuous dehydrogenation of formate salts in a flow-through reactor, it is impossible to make accurate predictions of how often catalyst bed would have to be regenerated. Based on the discussion presented in Section 3 of this Perspective, we suggest that the starting point for this process could be regeneration of the catalyst bed after every five bed-volumes of reactants fed to the reactor.

Different designs of reactors will also necessitate appropriate design of catalyst bed and form of the catalyst, which will account for change in flow of fluid, flow resistance, heat transfer, and multiple other variables. These factors as well as the scale of reaction will have to be taken into account during the engineering process.

5. Additional Considerations

A difficulty in any catalytic reaction is obtaining sufficient selectivity toward desired reaction. Selectivity of dehydrogenation of formate salts is very high and is only decreased by secondary decomposition of bicarbonate salt, which can produce small amounts of CO_2 (eq. 2)

$$2XHCO_3 \rightarrow X_2CO_3 + CO_2 + H_2O \qquad (eq. 2)$$

$$X = Li, Na, K, Cs, NH_4$$

The solubilities of bicarbonates are much lower than these of the formate salts (Table 4) [54], which would cause their precipitation in the reactor. Addressing this challenge would require an engineering solution, as discussed in previous section, and a novel reactor design to remove bicarbonate salts as they are formed.

Table 4 Solubilities of formate, bicarbonate and carbonate salts relevant to this Perspective [54].

Solubility (g/1000g H_2O)	Temperature (°C)					
	20	**30**	**40**	**60**	**80**	**100**
NH_4HCO_2	1430	x	2040	3110	5330	x
NH_4HCO_3	217	284	366	592	1090	3540
$NaHCO_2$	812	1020	1080	1220	1380	1600
$NaHCO_3$	96	111	127	160	196	236

Na$_2$CO$_3$	215	397	490	460	x	x
KHCO$_2$	3370	3610	3980	4710	5800	x
KHCO$_3$	337	399	475	656	x	x
K$_2$CO$_3$	1110	1140	1170	1270	x	x

x – not available.

We have already outlined in the introduction that the yield of hydrogen from formate salts is governed by the position of equilibrium (eq. 3).

$$HCOOX + H_2O \leftrightharpoons XHCO_3 + H_2 \qquad (eq. 3)$$

$$X = Li, Na, K, Cs, NH_4$$
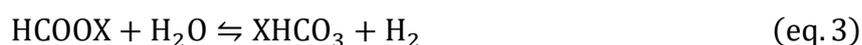
$$\triangle G° = -RTlnK \qquad (eq. 4)$$

From eq. 4 above, it can be seen that this equilibrium can be shifted by performing dehydrogenation of formate salts at elevated temperatures i.e., for these endothermic reactions, higher conversions and H$_2$ pressures could be obtained. This point is worth emphasizing, as we have also shown that various applications require different hydrogen feed rates (e.g., a backup power for data centers has different requirement than the continuous feed that need to be provided to microgrid). Therefore, it is not always necessary to release all the hydrogen at once and produce the highest pressure possible.

Considering the discussion outlined above, formate's aqueous nature, the high purity of released hydrogen, and low reaction temperature of dehydrogenation of formate salts, we can propose a use case where formate salt is used as competent H$_2$ carrier. Moreover, operation of fuel cells can provide low-grade heat, which may be sufficient for sustained evolution of H$_2$ from formate salts. Also, as PEM fuel cells operate in aqueous regime, water produced in the process could be used for dissolution of additional portion of the carrier (i.e., formate salt), which eliminates the need for additional costs associated with water transport.

6. Use Case Example

One potential application that has been investigated previously is the use of hydrogen in a microgrid application for seasonal storage [55]. In this study, 5.1 MT of hydrogen was proposed to be stored as compressed gas, which requires a total hydrogen storage volume of 1265 m^3 at 45 bar. As an alternative to compressed hydrogen, an aqueous solution of formate could be stored and converted to hydrogen as needed. To evaluate this scenario, we will assume the use of sodium formate, and that H$_2$ is produced during 5 months of summer for 8 hours *per* day and is used during 3 months of the winter at 12 hours *per* day. This results in an H$_2$ demand by fuel cell of 4.7 kg H$_2$/min, and by the reactor for rehydrogenation of bicarbonate to formate at 4.4 kg/min.

We assumed the reaction properties of dehydrogenation of sodium formate to sodium bicarbonate and its rehydrogenation reported by Koh *et al*. [28]. In this work, Pd catalyst was loaded on polyaniline (PANI)-derived mesoporous substrate that was pyrolyzed at 800 °C for 16

hours. The same catalyst was studied for both the hydrogenation and dehydrogenation reaction at 80 °C, differing only by the hydrogen pressure. At a pressure of 1 bar, Koh *et al.* achieved 50-55 % conversion of a 1 M formate solution to carbonate in approximately 120 minutes, limited by equilibrium. While at a pressure of 40 bar hydrogen, 82 % conversion of the 1 M bicarbonate to formate over 24 hours was reported.

Using the results reported in this article, the required volume of the fixed bed catalytic reactor and storage tanks can be estimated. For the calculation, the dehydrogenation reaction is assumed to be first order in formate salt and is conversion limited due to equilibrium. This reaction rate can be expressed as r = $k(C_f - C_c/K_{eq})$, where C_f is the concentration of formate, C_c is the concentration of carbonate, and K_{eq} is the equilibrium concentration as calculated by the van't Hoff equation (ΔH = 20.39 kJ/mol, ΔS = 59.9 J/mol/K). Using these assumptions, the reaction rate was fit to the experimental data and the reaction rate constant *k* was estimated as 3.2×10^{-4} mol/L tank/s. The dimensions of a fixed bed reactor for dehydrogenation at the required rate was calculated assuming the formate fractional conversion of the feed was 15 % and increased to 56 % in the reactor as shown in Table 5.

Table 5 Equipment sizing for a sodium formate/sodium bicarbonate reactor system for a seasonal hydrogen storage for a microgrid application.

Equipment Sizing (15-56% Conversion Formate)	Dimensions Assuming Solubility Limit $NaHCO_3$ @ 1.5 M (m^3)	Allowing Precipitation of Product @ 6 M (m^3)
Storage Tank	4857	1214
Dehydrogenation Reactor	15	3.7
Hydrogenation Reactor	32	8.1

A similar calculation was performed for hydrogenation. This reaction was also assumed to be first order with 85 % conversion in 24 hours. This reaction is much slower but is not limited by equilibrium constraints. As a result of the slow kinetics, the hydrogenation reactor is twice the size of the dehydrogenation reactor. Since both reactions will not be performed at the same time, only a single reactor is required, and its volume would be dictated by the larger volume requirements of the hydrogenation reaction.

We have also calculated total volume of the storage tanks required and the results indicate that if the concentration of the product and reactant are limited by the solubility limit of $NaHCO_3$ (~ 1.5 M), the required storage volume of formate is nearly 4 times the volume required for compressed hydrogen. However, if the bicarbonate could precipitate in the reactor without negative impact at a concentration of 6 M, parity with the volume of compressed hydrogen storage can be achieved. It is likely that in either case the capital cost of storage of the hydrogen as a formate will be significantly lower than the cost of storing compressed gaseous hydrogen.

In addition to the need for reactors, the formate/bicarbonate system will require approximately 33 kW of heat to maintain the reaction temperature during the endothermic dehydrogenation reaction. Because the reaction occurs at 80 °C, this could be provided by the fuel cell, or other low-grade heat source. Since periodic flushing of the catalyst column may be required to regenerate deactivated catalyst, this could either be done by having multiple reactors

in parallel such that one can be rinsed while others are operating, or a single reactor could be rinsed during the time period when it is not in use (12 hours/day for dehydrogenation and 16 hours/day for hydrogenation), as previously discussed.

7. Uncatalyzed Reactions

Though currently considered formate-based systems show great potential for reversible and controlled H_2 delivery, they are limited by catalyst decomposition, slower reaction kinetics, and dilution (due to low solubility of formate/bicarbonate in solvents). A literature survey showed that it is possible to decompose formate salts in the absence of catalyst and in the presence of water to form H_2 at T >250 °C [56, 57]. Although such uncatalyzed reaction has the potential to deliver high H_2 pressure and high volumetric hydrogen density, the gas stream is contaminated with CO_2 (eq. 5 below); for instance, at 350 °C the ratio between H_2 and CO_2 is 3.33:1 [56].

$$2HCOOX + H_2O \rightarrow 2H_2 + X_2CO_3 + CO_2 \qquad (eq. 5)$$
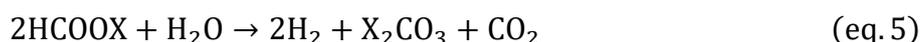
Since there is no catalyst used for this process, separation and catalyst costs are avoided. In addition, deliverable and usable hydrogen capacities are not limited by the solubility limit of sodium formate/bicarbonate/carbonate in water, as water exists in the gas phase at temperatures above 100 °C. The products, sodium carbonate and CO_2, can be hydrogenated back to sodium formate at relatively low temperature *via* thermal or electrocatalytic processes, achieving a carbon neutral cycle [7, 13, 16, 58-62]. However, the high energy requirement to dehydrogenate formate is a drawback that needs to be addressed for this uncatalyzed reaction.

8. Conclusions

We have presented the most pressing challenges that need to be addressed if formate salts are to be used as hydrogen carriers. The most promising features of formate salts are their stability and non-toxicity. While stability may be viewed as a drawback during fast H_2 delivery, it is crucial for long term agnostic energy storage, as it minimizes H_2 loses. While the H_2 is mainly stored in pressurized vessels, other storage methods include liquefaction of H_2 and/or storage in salt caverns, and they all include significant loss of H_2. Additionally, use of formate salts as hydrogen carriers may provide steady, long term release of high purity H_2 gas from aqueous media, which would be appropriate for applications where rapid release rates are not deciding factor. As the active catalysts are crucial to release of H_2 from formate salts, it is imperative to understand modes of their deactivation and devise pathways for preventing loss of activity. In this article, we have outlined the most common observations of factors that lead to deactivation of Pd catalysts and presented prospective engineering solutions that can be adapted to facilitate recycling of the catalyst. We note that while there is no consensus as to how Pd catalyst is deactivated, promising results of immobilization of Pd nanoparticles outlined by Song *et al*. and frequent catalyst washing offer a viable pathway for avoiding deactivation of the catalyst [36].

Author Contributions

All authors contributed evenly to this work.

Funding

Competing Interests

The authors have declared that no competing interests exist.

References

1. Pivovar B, Rustagi N, Satyapal S. Hydrogen at scale (H_2@Scale): Key to a clean, economic, and sustainable energy system. Electrochem. Soc Interface. 2018; 27: 47.
2. Niermann M, Drünert S, Kaltschmitt M, Bonhoff K. Liquid organic hydrogen carriers (LOHCs) – Techno-economic analysis of LOHCs in a defined process chain. Energy Environ Sci. 2019; 12: 290-307.
3. Home - The Advanced Hydrogen Energy Chain Association for Technology Development (AHEAD). Yokohama: The Advanced Hydrogen Energy Chain Association for Technology Development. Available from: https://www.ahead.or.jp/en.
4. Brückner N, Obesser K, Bosmann A, Teichmann D, Arlt W, Dungs J, et al. Evaluation of industrially applied heat-transfer fluids as liquid organic hydrogen carrier systems. ChemSusChem. 2014; 7 :229-235.
5. Anouar A, Katir N, El Kadib A, Primo A, Garcia H. Palladium supported on porous chitosan-graphene oxide aerogels as highly efficient catalysts for hydrogen generation from formate. Molecules. 2019; 24: 3290.
6. Dobrovolná Z, Červený L. Ammonium formate decomposition using palladium catalyst. Res Chem Intermediat. 2000; 26: 489-497.
7. Bi QY, Lin JD, Liu YM, Du XL, Wang JQ, He HY, et al. An aqueous rechargeable formate-based hydrogen battery driven by heterogeneous Pd catalysis. Angew Chem Int Ed Engl. 2014; 53: 13583-13587.
8. Wiener H, Zaidman B, Sasson Y. Storage of energy by solutions of alkali formate salts. Sol Energy. 1989; 43: 291-296.
9. Wiener H, Sasson Y, Blum J. Palladium-catalyzed decomposition of aqueous alkali metal formate solutions. J Mol Catal. 1986; 35: 277-284.
10. Wang J, Tan H, Jiang D, Zhou K. Enhancing H_2 evolution by optimizing H adatom combination and desorption over Pd nanocatalyst. Nano Energy. 2017; 33: 410-417.
11. Wang F, Xu J, Shao X, Su X, Huang Y, Zhang T. Palladium on nitrogen-doped mesoporous carbon: A bifunctional catalyst for formate-based, carbon-neutral hydrogen storage. ChemSusChem. 2016; 9: 246-251.

12. Zhu X, Du L, Guo Z, Chen S, Wu B, Liu X, et al. Tandem catalysis induced by hollow PdO: Highly efficient H_2 generation coupled with organic dye degradation via sodium formate reforming. Catal Sci Technol. 2018; 8: 6217-6227.

13. Su J, Yang L, Lu M, Lin H. Highly efficient hydrogen storage system based on ammonium bicarbonate/formate redox equilibrium over palladium nanocatalysts. ChemSusChem. 2015; 8: 813-816.

14. Wang WH, Himeda Y, Muckerman JT, Manbeck GF, Fujita E. CO_2 hydrogenation to formate and methanol as an alternative to photo- and electrochemical CO_2 reduction. Chem Rev. 2015; 115: 12936-12973.

15. Álvarez A, Bansode A, Urakawa A, Bavykina AV, Wezendonk TA, Makkee M, et al. Challenges in the greener production of formates/formic acid, methanol, and DME by heterogeneously catalyzed CO_2 hydrogenation processes. Chem Rev. 2017; 117: 9804-9838.

16. Bulushev DA, Ross JR. Heterogeneous catalysts for hydrogenation of CO2 and bicarbonates to formic acid and formates. Catal Rev. 2018; 60: 566-593.

17. Ceballos BM, Yang JY. Highly selective electrocatalytic CO_2 reduction by $[Pt(dmpe)_2]^{2+}$ through kinetic and thermodynamic control. Organometallics. 2020; 39: 1491-1496.

18. Cunningham DW, Barlow JM, Velazquez RS, Yang JY. Reversible and selective CO_2 to HCO_2^- electrocatalysis near the thermodynamic potential. Angew Chem Int Ed Engl. 2020; 59: 4443-4447.

19. Cunningham DW, Yang JY. Selective electrocatalytic reduction of CO_2 to HCO_2^-. Trends Chem. 2020; 2: 401-402.

20. Grubel K, Jeong H, Yoon CW, Autrey T. Challenges and opportunities for using formate to store, transport, and use hydrogen. J Energy Chem. 2020; 41: 216-224.

21. Dr. Vincent Chevrier Presents in "Ironmaking with Alternative Reductants" Webinar by AIST. North Carolina: MIDREX; 2020. Available from: https://www.midrex.com/story/dr-vincent-chevrier-presents-in-ironmaking-with-alternative-reductants-webinar-by-aist/.

22. Advancing the Landscape of Clean Energy Innovation. Washington: Energy Futures Initiative; 2019. Available from: https://energyfuturesinitiative.org/news/2019/2/6/clean-energy-innovation-report.

23. Fischedick M, Marzinkowski J, Winzer P, Weigel M. Techno-economic evaluation of innovative steel production technologies. J Clean Prod. 2014; 84: 563-580.

24. Sodium Formate Market (Application: Food Additives, Agriculture, Textile & Printing, Aerospace, and Others) - Global Industry Analysis, Size, Share, Growth, Trends, and Forecast, 2019-2027[Internet]. Albany: Transparency Market Research; 2019. Available from: https://www.transparencymarketresearch.com/sodium-formate-market.html.

25. Awane Y, Otsuka S, Nagata M, Tanaka F. Process for the continous production of highly pure sodium formate patent. US3928435A. 1973.

26. 2019 Integrated Energy Policy Report. Sacramento: California Energy Commission; 2019. Available from: https://www.energy.ca.gov/data-reports/reports/integrated-energy-policy-report/2019-integrated-energy-policy-report.

27. DOE Technical Targets for Hydrogen Production from Electrolysis. Washington: Energy Efficiency & Renewable Energy; 2020. Available from: https://www.energy.gov/eere/fuelcells/doe-technical-targets-hydrogen-production-electrolysis.

28. Koh K, Jeon M, Chevrier DM, Zhang P, Yoon CW, Asefa T. Novel nanoporous N-doped carbon-supported ultrasmall Pd nanoparticles: Efficient catalysts for hydrogen storage and release. Appl Catal B-Environ. 2017; 203: 820-828.

29. Minami Y, Amao Y. Catalytic mechanism for selective hydrogen production based on formate decomposition with polyvinylpyrrolidone-dispersed platinum nanoparticles. Sustain Energy Fuels. 2020; 4: 3458-3466.

30. Boechler AN. Hydrogen interaction with platinum and palladium surfaces. Oregon: Oregon State University; 2019.

31. Jones S, Kolpin A, Tsang SC. Modification of Pd for formic acid decomposition by support grafted functional groups. Catal Struct React. 2014; 1: 19-24.

32. Wang Q, Tsumori N, Kitta M, Xu Q. Fast dehydrogenation of formic acid over palladium nanoparticles immobilized in nitrogen-doped hierarchically porous carbon. ACS Catal. 2018; 8: 12041-12045.

33. Li Z, Yang X, Tsumori N, Liu Z, Himeda Y, Autrey T, et al. Tandem nitrogen functionalization of porous carbon: Toward immobilizing highly active palladium nanoclusters for dehydrogenation of formic acid. ACS Catal. 2017; 7: 2720-2724.

34. Hwang YJ, Kwon Y, Kim Y, Sohn H, Nam SW, Kim J, et al. Development of an autothermal formate-based hydrogen generator: From optimization of formate dehydrogenation conditions to thermal integration with fuel cells. ACS Sustain Chem Eng. 2020; 8: 9846-9856.

35. Hammond C. Intensification studies of heterogeneous catalysts: Probing and overcoming catalyst deactivation during liquid phase operation. Green Chem. 2017; 19: 2711-2728.

36. Song FZ, Zhu QL, Tsumori N, Xu Q. Diamine-alkalized reduced graphene oxide: Immobilization of sub-2 nm palladium nanoparticles and optimization of catalytic activity for dehydrogenation of formic acid. ACS Catal. 2015; 5: 5141-5144.

37. Hansen TW, Delariva AT, Challa SR, Datye AK. Sintering of catalytic nanoparticles: Particle migration or Ostwald ripening? Acc Chem Res. 2013; 46: 1720-1730.

38. McNaught AD. Compendium of chemical terminology. 2nd ed. Oxford: Blackwell Scientific Publications; 1997.

39. Douidah A, Marécot P, Labruquère S, Barbier J. Stability of supported platinum catalysts in aqueous phase under hydrogen atmosphere. Appl Catal A Gen. 2001; 210: 111-120.

40. Ravenelle RM, Copeland JR, Kim WG, Crittenden JC, Sievers C. Structural changes of γ-Al$_2$O$_3$-supported catalysts in hot liquid water. ACS Catal. 2011; 1: 552-561.

41. Vilcocq L, Cabiac A, Especel C, Lacombe S, Duprez D. Study of the stability of Pt/SiO$_2$–Al$_2$O$_3$ catalysts in aqueous medium: Application for sorbitol transformation. Catal Commun. 2011; 15: 18-22.

42. Yamakata A, Kubota J, Kondo JN, Hirose C, Domen K, Wakabayashi F. In situ observation of the dehydration of formate on Ni(110). J Phys Chem B. 1997; 101: 5177-5181.

43. Shin DY, Kim MS, Kwon JA, Shin YJ, Yoon CW, Lim DH. Fundamental mechanisms of reversible dehydrogenation of formate on N-Doped graphene-supported Pd nanoparticles. J Phys Chem C. 2018; 123: 1539-1549.

44. Li N, Ma X, Zha Q, Kim K, Chen Y, Song C. Maximizing the number of oxygen-containing functional groups on activated carbon by using ammonium persulfate and improving the temperature-programmed desorption characterization of carbon surface chemistry. Carbon. 2011; 49: 5002-5013.

45. Su J, Yang L, Yang X, Lu M, Luo B, Lin H. Simultaneously converting carbonate/bicarbonate and biomass to value-added carboxylic acid salts by aqueous-phase hydrogen transfer. ACS Sustain Chem Eng. 2015; 3: 195-203.

46. Dillon AC, Heben MJ. Hydrogen storage using carbon adsorbents: Past, present and future. Appl Phys A. 2001; 72: 133-142.

47. Anson A, Lafuente E, Urriolabeitia E, Navarro R, Benito AM, Maser WK, et al. Hydrogen capacity of palladium-loaded carbon materials. J Phys Chem B. 2006; 110: 6643-6648.

48. De la Casa-Lillo MA, Lamari-Darkrim F, Cazorla-Amorós D, Linares-Solano A. Hydrogen storage in activated carbons and activated carbon fibers. J Phys Chem B. 2002; 106: 10930-10934.

49. Caiti M, Padovan D, Hammond C. Continuous production of hydrogen from formic acid decomposition over heterogeneous nanoparticle catalysts: From batch to continuous flow. ACS Catal. 2019; 9: 9188-9198.

50. Dufresne P. Hydroprocessing catalysts regeneration and recycling. Appl Catal A-Gen. 2007; 322: 67-75.

51. Song Y, Liu S, Wang Q, Xu L, Zhai Y. Coke burning behavior of a catalyst of ZSM-5/ZSM-11 co-crystallized zeolite in the alkylation of benzene with FCC off-gas to ethylbenzene. Fuel Process Technol. 2006; 87: 297-302.

52. Li Y, Zhang C, Liu Y, Tang S, Chen G, Zhang R, et al. Coke formation on the surface of Ni/HZSM-5 and Ni-Cu/HZSM-5 catalysts during bio-oil hydrodeoxygenation. Fuel. 2017; 189: 23-31.

53. Schipper PH, Krambeck FJ. A reactor design simulation with reversible and irreversible catalyst deactivation. Chem Eng Sci. 1986; 41: 1013-1019.

54. Dean JA. Lange's Handbook of Chemistry. 15th ed. New York: McGraw-Hill; 1999.

55. Pauksztat A, Saliger R, Boyanov N. Residential energy supply concept with integration of renewable energies and energy storage. Chem Eng Technol. 2019; 42: 1907-1913.

56. Onwudili JA, Williams PT. Hydrothermal reactions of sodium formate and sodium acetate as model intermediate products of the sodium hydroxide-promoted hydrothermal gasification of biomass. Green Chem. 2010; 12: 2214-2224.

57. Garcia-Verdugo E, Liu Z, Ramirez E, Garcia-Serna J, Fraga-Dubreuil J, Hyde JR, et al. In situ generation of hydrogen for continuous hydrogenation reactions in high temperature water. Green Chem. 2006; 8: 359-364.

58. Kothandaraman J, Czaun M, Goeppert A, Haiges R, Jones JP, May RB, et al. Amine-free reversible hydrogen storage in formate salts catalyzed by ruthenium pincer complex without pH control or solvent change. ChemSusChem. 2015; 8: 1442-1451.

59. Boddien A, Gartner F, Federsel C, Sponholz P, Mellmann D, Jackstell R, et al. CO_2-"neutral" hydrogen storage based on bicarbonates and formates. Angew Chem Int Ed Engl. 2011; 50: 6411-6414.

60. Loges B, Boddien A, Junge H, Beller M. Controlled generation of hydrogen from formic acid amine adducts at room temperature and application in H_2/O_2 fuel cells. Angew Chem Int Ed Engl. 2008; 47: 3962-3965.

61. Papp G, Csorba J, Laurenczy G, Joó F. A charge/discharge device for chemical hydrogen storage and generation. Angew Chem Int Ed Engl. 2011; 50: 10433-10435.

62. Hsu SF, Rommel S, Eversfield P, Muller K, Klemm E, Thiel WR, et al. A rechargeable hydrogen battery based on Ru catalysis. Angew Chem Int Ed Engl. 2014; 53: 7074-7078.

Enjoy *JEPT* by:

1. Submitting a manuscript
2. Joining in volunteer reviewer bank
3. Joining Editorial Board
4. Guest editing a special issue

For more details, please visit:
http://www.lidsen.com/journal/jept